Received: 28 December 2018 | Revised: 4 March 2019 | Accepted: 11 March 2019

DOI: 10.1002/aoc.4929

WILEY Applied Organometallic Chemistry

FULL PAPER

Cooperative effect through different bridges in nickel catalysts for polymerization of ethylene

Mostafa Khoshsefat[1,2] | Abbas Dechal[2] | Saeid Ahmadjo[2] | S. Mohammad M. Mortazavi[2] | Gholamhossein Zohuri[3] | Joao B.P. Soares[1]

[1]Department of Chemical and Materials Engineering, University of Alberta, Edmonton, Alberta T6G 1H9, Canada

[2]Department of Catalysis, Iran Polymer and Petrochemical Institute (IPPI), PO Box 14965/115, Tehran, Iran

[3]Department of Chemistry, Faculty of Science, Ferdowsi University of Mashhad, PO Box 91775, Mashhad, Iran

Correspondence
Saeid Ahmadjo, Department of Catalysis, Iran Polymer and Petrochemical Institute (IPPI), PO Box 14965/115, Tehran, Iran.
Email: s.ahmadjo@ippi.ac.ir

A series of mononuclear (M_1 and M_2) and dinuclear (C_1–C_6) Ni α-diimine catalysts activated by modified methylaluminoxane were used in polymerization of ethylene. Catalyst C_2 bearing the optimum bulkiness showed the highest activity (1.6×10^6 g PE (mol Ni)$^{-1}$ h^{-1}) and the lowest short-chain branching (32.5/1000 C) in comparison to the dinuclear and mononuclear analogues. Although the mononuclear catalysts M_1 and M_2 polymerized ethylene to a branched amorphous polymer, the dinuclear catalysts led to different branched semicrystalline polyethylenes. Homogeneity and heterogeneity in the microstructure of the polyethylene samples was observed. Different trends for each catalyst were assigned to *syn* and *anti* stereoisomers. In addition, thermal behavior of the samples in the successive self-nucleation and annealing technique exhibited different orders and intensities from methylene sequences and lamellae thickness in respect of each stereoisomer behavior. Higher selectivity of hexyl branches obtained by catalyst C_2 showed a cooperative effect between the centers. The results also revealed that for catalysts C_5 and C_6, selectivity of methyl branches led to very high endotherms and crystalline sequences with melting temperatures higher than that of 100% crystalline polyethylene indicating ethylene/propylene copolymer analogues. For catalysts C_3 and C_4, more vinyl end groups were a result of the long distance between the Ni centers. Kinetic profiles of polymerization along with a computational study of the precatalysts and catalysts demonstrated that there is a direct relation between rate constant, energy interval of catalyst and precatalyst, and interaction energy of Et···methyl cationic active center (Et···MCC or π–Comp.). Based on this, narrow energy interval (activation energy) of precatalyst and catalyst leads to fast and higher activation rate (catalyst M_2), and strong interaction of ethylene and catalyst leads to high monomer uptake and productivity (catalyst C_2). Moreover, theoretical parameters including electron affinity, Mulliken charge on Ni, chemical potential and hardness, and global electrophilicity showed optimum values for C_2.

KEYWORDS
bridge, cooperative effect, dinuclear catalyst, ethylene–propylene analogue, nickel

1 | INTRODUCTION

The main purposes in synthesis of multinuclear catalysts are superior activity and selectivity.[1] In the field of multinuclear catalysts for polymerization of olefins, many studies have been reported. In some cases, a unique polymer with a distinct microstructure and narrow polydispersity is obtained.[2–5] However, in other cases, a broad to bimodal molecular weight distribution has been reported.[6–9] Higher or lower activity and selectivity of multinuclear catalysts in comparison to mononuclear ones can be attributed to the presence of adjacent metal centers or the ligand structure, all of which effects could be interpreted as steric and electronic effects.[1] Each structural parameter has an impact on the catalyst behavior. To clarify, when two centers in a dinuclear catalyst are similar and far enough from each other, one can observe behavior similar to that of the mononuclear analogue. However, if the centers be at an effective distance so as to have an interaction, the scenario could change. Moreover, the interactions can be positive or negative, giving cooperative or competitive effects.

The effective distance between two centers basically depends on the nature of the centers and ligand structure. The possible interactions between a monomer/polymer chain and the second center are dependent on monomer length and presence of weakly basic substituents such as hydrogen or phenyl in the monomer. On the other hand, the nature and length of the linker between the two centers are crucial.[10–12] Whereas a rigid bridge poses the centers at a constant distance, a flexible one could lead to variable distance. Bridges of various structures (polymethylene, phenylene, silane, siloxane, rigid/flexible) in multinuclear metallocene and constrained geometry complex-based catalysts have been used and reported, although in the field of late transition metal catalysts, there are more scarce reports.[13–16]

Based on this, there is a demand for the study of the effect of length and nature of bridge and substituents in multinuclear late transition metal catalysts. The importance of late transition metal catalysts especially Ni and Pd complexes is in regard to chain walking mechanism and their activity in the copolymerization of polar monomers and production of highly branched polyolefins and thermoplastic elastomers.[17–26] This shows the importance of catalyst structure that strongly affects the resulting polymer microstructure.[27–35] Based on this, dinuclearity effect can control this behavior through the different structures. For instance, Jesús and co-workers reported a dendritic complex bearing low-stericity *ortho*-aryliminopyridine ligands which were active for production of a mixture of oily and solid polyethylene.[36] Chen and co-workers reported a rigid conjugated α-diimine backbone in dinuclear Ni and Pd catalysts, and unimodal to bimodal molecular weight distributions of polyethylene were observed.[37] A series of symmetric to unsymmetric bimetallic Ni complexes bearing aryl-linked iminopyridines affording mixtures of waxes and low-molecular-weight solid polyethylene were reported by Solan and co-workers.[38] Sun and co-workers synthesized a series dinuclear iminopyridine Ni complexes bearing rigid and rigid/flexible bridges giving oligomeric to oligomeric/polymeric polyethylene.[39,40] Moreover, they reported a series of α-diimine dinuclear catalysts with higher activity and the resultant polyethylene had high molecular weight and branching density.[41] Structures of flexible/rigid bridges reported by Luo and Schumann were active in ethylene polymerization but microstructural properties of products were not mentioned.[42] In addition, we reported a series of dinuclear α-diimine Ni-based catalysts with structures having higher electronic and steric effects that showed higher activity, although molecular weight distribution was broad.[43]

In addition to practical reports, there are some computational studies of catalyst structure and polymerization that we used as inputs of our calculations.[43–48] In the work reported herein, we computed the structures for better understanding of relation between theoretical parameters, interactions and catalyst behaviors. Altogether, by considering all previous reports of dinuclear Ni-based catalysts, the structural properties of the bridges need more investigations. Based on this, we studied the effect of the nature and length of spacer between two Ni centers in dinuclear α-diimine-based catalysts. The catalyst behavior and the resultant polymers obtained in the presence of these complexes and mononuclear analogues using modified methylaluminoxane (MMAO) were investigated. Moreover, theoretical calculation was used to confirm and explain the kinetic profiles and catalyst behavior.

2 | EXPERIMENTAL

2.1 | Materials

All manipulations of air-/water-sensitive compounds were conducted under argon/nitrogen atmosphere using standard Schlenk techniques. All solvents were purified prior to use. Toluene (purity 99.9%) was purified over sodium wire/benzophenone, and used as polymerization medium. Ethylene (purity 99.99%) was provided by Bandar Imam Petrochemical Company (BIPC, Iran). MMAO (7 wt% in toluene) was supplied by Sigma Aldrich Chemicals (Steinheim, Germany).

2.2 | Polymerization procedure

Ethylene polymerizations were conducted in a 200 ml stainless steel Buchi reactor, using toluene as the solvent. The reactor was purged with nitrogen at 90°C for 2 h prior to each reaction. Dried toluene was introduced under nitrogen atmosphere, followed by MMAO and catalyst. The reactor was saturated with ethylene to the desired total pressure and reaction proceeded for 30 min, by mixing at 800 rpm. To better study the reaction coordinate, the stirrer was stopped during injection of catalyst then stirrer and plot started, concurrently. Ethylene consumption was compensated using a mass flow meter to keep the pressure constant. Finally, the reactor was evacuated and the product was washed with acidic methanol (5%) and dried under reduced pressure.

2.3 | Characterization

Fourier transform infrared (FT-IR) spectra were obtained using Bruker AC-400 and Thermo Nicolet AVATAR 370 spectrometers. Molecular weight distributions (MWDs) were determined with a Polymer Char high-temperature gel permeation chromatography (GPC) instrument, run at 145°C under a flow of 1,2,4-trichlorobenzene at a rate of 1 ml min^{-1}. The GPC instrument was equipped with three detectors in series (IR, light scattering and differential viscometer) and calibrated with narrow polystyrene standards.[49] ^{13}C NMR spectra of polyethylene were recorded with a Bruker AC-400 MHz instrument at 115°C in deuterated tetrachloroethane with tetramethylsilane as an internal standard. Differential scanning calorimetry (DSC) thermograms were recorded inthe second heating cycle with a rate of 10°C min^{-1} using a PerkinElmer DSC Q100 instrument. Successive self-nucleation and annealing (SSA) analysis was carried out at heating and cooling rates of 10°C min^{-1}. Samples were first heated to 180°C, maintained for 10 min and cooled to 25°C. Subsequently, samples were heated to the first self-nucleation temperature, maintained for 10 min then cooled to 25°C. Successive self-nucleation was achieved by repeatedly heating to the next self-nucleation temperature and cooling to 25°C. After covering the temperature range between 165 and 25°C, the final heating ramp from 25 up to 190°C was applied to collect all melting endotherms.[50]

2.4 | Ligands and complex synthesis

All the ligands and complexes were synthesized and characterized as fully described in our recent papers.[51,52] The catalysts studied were mononuclear (M_1 and M_2) and dinuclear (C_1–C_6) Ni α-diimine-based catalysts.

3 | RESULTS AND DISCUSSION

3.1 | Ethylene polymerization catalyzed by mononuclear and dinuclear catalysts

The results of ethylene polymerization showed the highest catalyst activity of C_2 among the dinuclear and mononuclear catalysts in the order of $C_2 > M_2 > M_1 > C_4 > C_3 > C_1 > C_6 > C_5$ (Figure 1). Catalyst C_2 has the optimum bulkiness around the active center (methyl and isopropyl on the *ortho* position of aryl rings) which is called the "*ortho*-aryl effect".[53] This effect also implies the steric and electronic impacts of ligand architecture and metal center. The kinetic profiles of polymerization (Figure 2) demonstrate ethylene consumption for dinuclear complexes, and the structures with more electron-rich groups and substituents (phenyl and &bond;CH_2&bond; units) as a bridge exhibited greater activity and ethylene uptake. The effect of backbone was observed for catalysts M_2 and C_4 in comparison to M_1 and C_3, respectively. Higher activity of M_2 than M_1 is consistent on our previous results for higher α-olefin polymerization.[52] This suggested that the presence of acenaphthene could make the active center to be a better π-acceptor. This trend along with the *ortho*- aryl effect of catalyst C_2 made it the most effective and stable catalyst. Lower Mulliken charge on Ni atom(s) in MCC (Figure 3b) indicated electronic effects of the ligand structure on the active center(s). This can be observed in comparison of M_2 versus M_1, C_2 versus C_1, C_4 versus C_3 and C_6 versus C_5.

Activation of the complexes is fast followed by reaching high values of ethylene uptake, propagation, chain transfers, termination and deactivation reactions (Figure 2).[54] It has been reported that the rate-determining step in polymerization of ethylene is chain growth while for higher α-olefins it is monomer trapping.[54,55] The rate of each step depends on the catalyst structure and polymerization conditions. Although the steep slope at the beginning of the kinetic profile represents a fast activation and strong monomer coordination (Equations (1)–(23)), the trend of the profile highlights the activity through a longer time. The chemical equations are

$$C + Al \rightarrow C^{*} \; Activation \tag{1}$$

$$P_r + M \rightarrow P_{r+1} \begin{cases} r = 0 \rightarrow P_0 = C^{*} \; Coordination \\ r > 0 \qquad\qquad\quad Propagation \end{cases} \tag{23}$$

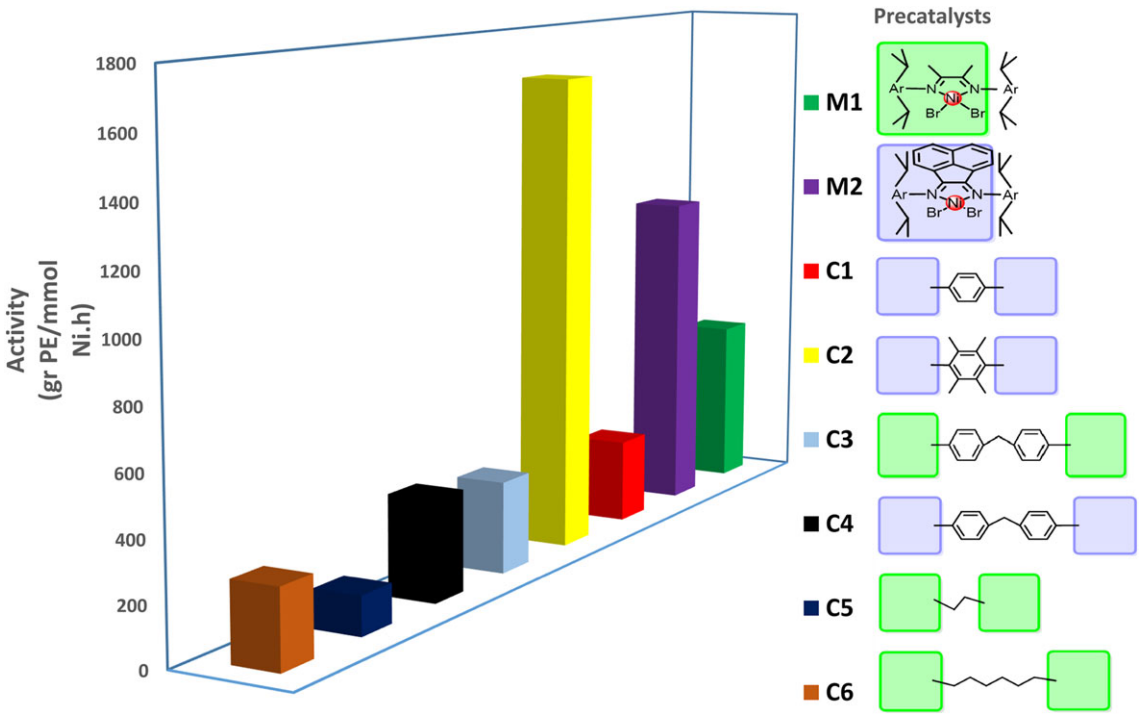

FIGURE 1 Bar chart of activities of mononuclear (M_1 and M_2) and dinuclear (C_1–C_6) catalysts

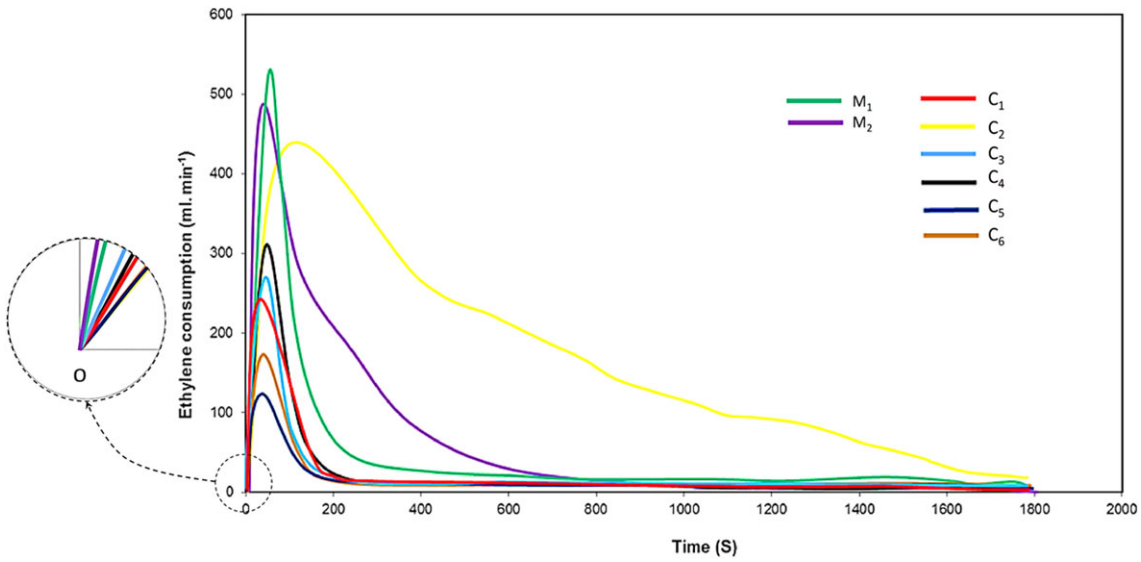

FIGURE 2 Kinetic profiles of ethylene polymerization using mononuclear (M_1 and M_2) and dinuclear (C_1–C_6) catalysts

$$P_r + T \rightarrow P_1 + D_r \quad Chain transfer \tag{4}$$

$$P_r \rightarrow C_d + D_r \quad deactivation \tag{5}$$

where C is the metal center, Al is the cocatalyst and C* is the active center (catalyst). P_r is equivalent to C* for the first insertion of monomer, M represents the ethylene monomer and P_{r+1} is the growing polymer chain. In the chain transfer equation, T is the chain transfer species which can be the cocatalyst, catalyst, monomer and chain transfer agents (such as H_2). D_r is the dead polymer and C_d is the deactivated site. Since the reactions were carried out under similar conditions, the effects of structure on polymerization kinetics revealed that optimum bulkiness in architecture of catalyst leads to efficient shielding of axial sites of active centers against deactivation and chain transfer reactions (Equations (4) and (5)). As the first step in the ethylene insertion process is formation of a π-Comp. and the most

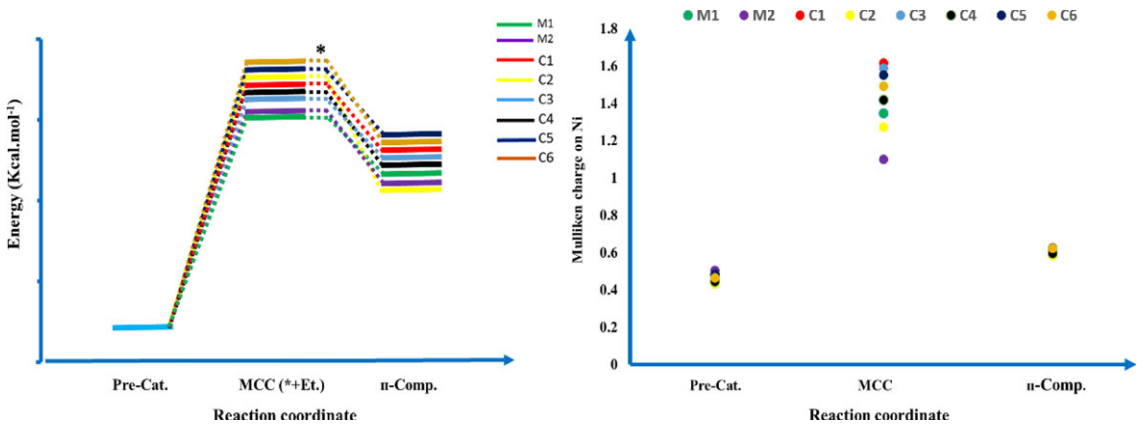

FIGURE 3 (a) Relative energy profiles for Pre-Cat., MCC and π-Comp. (b) Mulliken charge on Ni in mononuclear and dinuclear structures

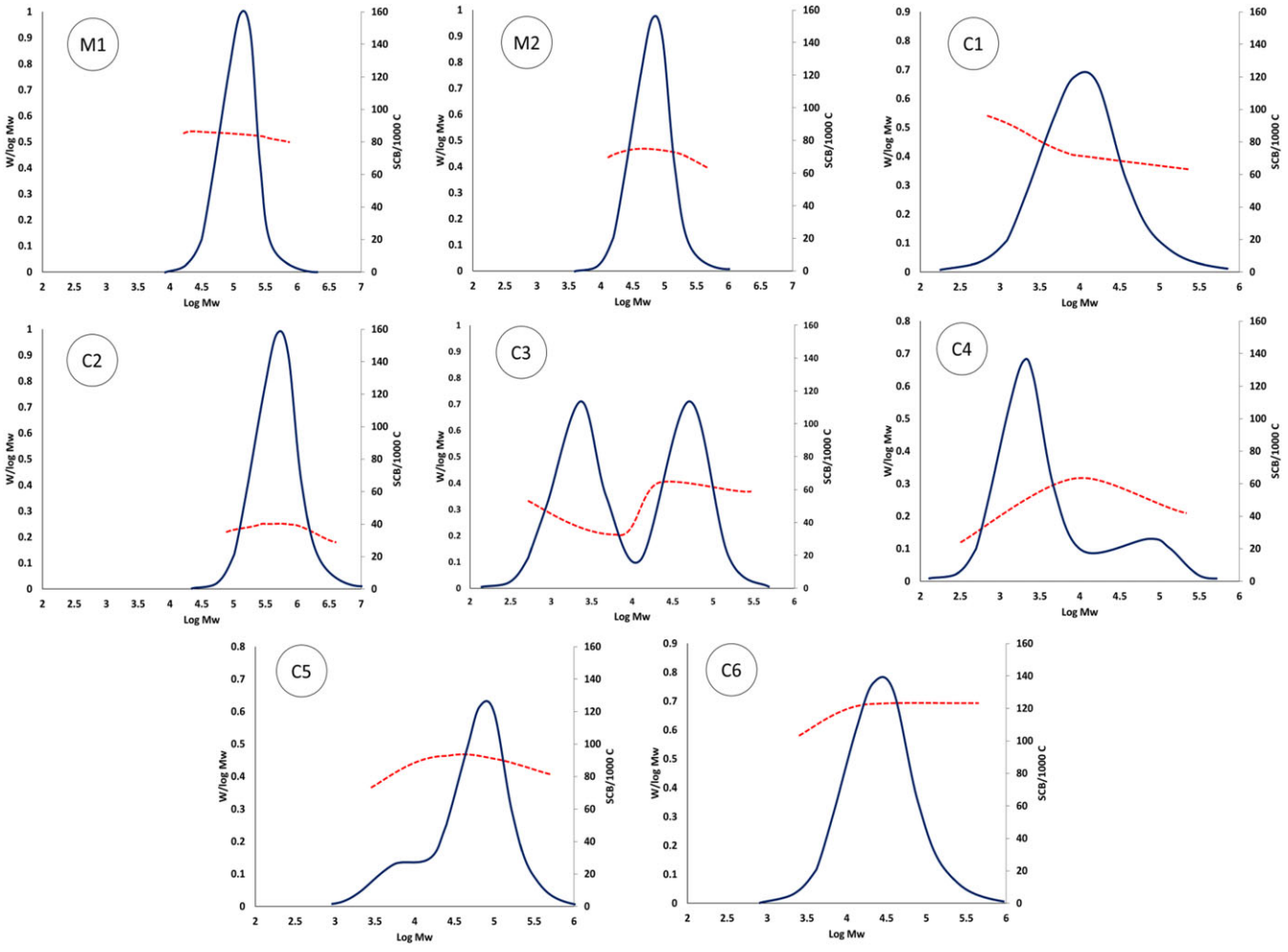

FIGURE 4 MWD and SCB curves of polyethylene obtained using mononuclear and dinuclear catalysts

stable structure is found, the ethylene monomer is oriented in a direction perpendicular to the MCC.[45]

Although the narrow energy interval (Figure 3) between the precatalyst and catalyst (lower activation energy) led to faster activation (K_a) and coordination for catalyst M_2 having lower steric and electronic effects, catalyst C_2 through optimum bulkiness, synergistic effect and higher stability showed higher K_p/K_{tr} and K_p/K_d rates. It was also mentioned before that the rate-determining step of reaction is chain growth where the

TABLE 1 Results of ethylene polymerization using mononuclear (M_1 and M_2) and dinuclear (C_n, n = 1–6) catalysts[a]

Sample	Catalyst	Yield (g)	Activity (× 10^6 g PE (mol Ni)$^{-1}$ h^{-1})	M_n (g mol^{-1})[c]	M_w (g mol^{-1})[c]	MWD[c]	T_m (°C)[b]	X_c (%)[b]	CH_3 (per 1000 C)[c]	C&dbond;C (per 1000 C)[c]
1	M1	2.43	1.16	58 700	104 000	1.8	—	—	81.4	—
2	M2	4.67	2.22	51 700	112 200	2.2	45.0	<0.1	66.3	—
3	C1	1.21	0.58	1 900	34 000	17.9	123.0	22.0	57.2	—
4	C2	6.90	3.28	207 000	501 000	2.4	121.0	24.7	32.5	—
5	C3	1.32	0.63	3 100	142 000	45.8	134.9	1.8	48.7	0.3
6	C4	1.45	0.69	2 100	58 000	27.6	105.1	40.5	34.3	0.5
7	C5	0.56	0.27	30 000	246 000	8.2	145.7	26.9	151.1	—
8	C6	1.12	0.53	24 000	148 000	6.2	145.4	20.0	287.6	—
9[d]	C2	5.19	2.47	114 000	352 000	3.1	119.1	20.4	39.9	—
10[e]	C2	3.44	1.64	46 000	225 000	4.9	118.5	14.9	45.6	0.1
11[f]	C2	10.57	5.03	66 000	256 000	3.9	120.6	19.8	35.1	—

[a]Polymerization conditions: [Al/Ni] = 1500, monomer pressure (M_p), 1.5 bar; polymerization time, 30 min; toluene, 80 ml; polymerization temperature (T_p), 26°C; [Ni] = 4.2 μmol.

[b]Determined using DSC.

[c]Determined using GPC-IR.

[d]T_p = 45°C.

[e]T_p = 65°C.

[f]T_p = 65°C and M_p = 4.5 bar.

active center reacts with the monomer. The higher energy of monomer binding to the active metal center in the propagation step (for C_2) could lead to higher rate of propagation/termination or chain transfer (K_p/K_{tr}), and abrupt decreasing of kinetics profile for the other dinuclear catalysts is due to less shielding effect and lower monomer binding energy. Although the mononuclear catalysts showed higher monomer uptake, the activities decreased faster at longer time in comparison to C_2 which can be attributed to the higher stability of dinuclear catalyst C_2 in comparison to the mononuclear catalysts, as well. These results also are consistent with our previous reports on polymerization of longer α-olefins.[51]

Polymerization at higher temperature (45 and 65°C) showed a moderate thermal stability of catalyst C_2. Moreover, increasing temperature led to an increase of branching density and MWD and lower T_m, crystallinity and molecular weight. These observations are due to the enhancing of chain transfer reactions and formation of branches where the increasing temperature could stabilize the second stereoisomer affording the broad MWD.[43,51,53] Higher monomer pressure at high temperature of polymerization (run 11) afforded a higher yield of polyethylene with higher molecular weight and degree of crystallinity. Greater concentration of ethylene leading to more insertions was the reason for these results.[43,51]

3.2 | Microstructural properties

Molecular weight and MWD of mononuclear catalysts (M_1 and M_2) correspond to their single-site feature of the center, while for dinuclear catalysts, the presence of stereoisomers afforded different trends in polymerization pathway and products as can be observed in the GPC and short-chain branching (SCB) curves (Figure 4). Ascending or descending SCB trends as a function of molecular weight (dinuclear catalysts except C_2) showed the stereoisomer activities in polymerization media through different steric and electronic effects around the active center (Figure 4). The extent of broadening in MWD can be related to the difference between two stereoisomers and structural properties. To clarify, according to the computational results for C_5 and C_6, as the structural differences between two stereoisomers (*syn* and *anti*) are less, variations in polymerization pathway (SCB curves) and final product are minor, and the distributions are much narrower in comparison to C_1, C_3 and C_4 (Table 1).

Both branching density and distribution of the samples obtained using mononuclear catalysts (M_1 and M_2) in comparison to dinuclear catalysts are different. It can be suggested that each stereoisomer is responsible for producing low- or high-molecular-weight fraction of polymer and particular microstructure. Increasing or decreasing in SCBs as a function of molecular weight was observed.

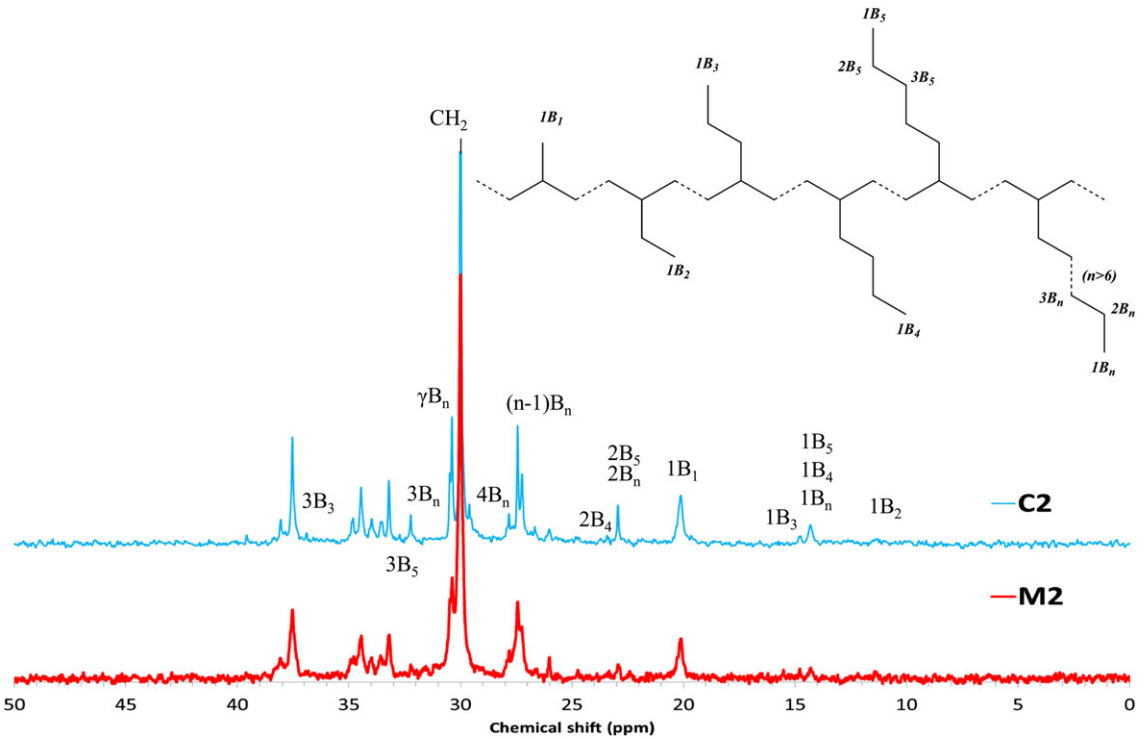

FIGURE 5 ^{13}C NMR spectra of samples obtained using catalysts M_2 and C_2

Branch formation pathway consists of β-H elimination and reinsertion, indicating that the steric and electronic effects of backbone and bridge along with the nuclearity control the behavior of the catalyst. Based on this, the SCB formation, although by M_1 is decreasing and also for all the catalysts, SCB trend is decreasing, the changes in the SCB curves except M_1, M_2 and C_2 are significant. In addition, the effect of backbone on the catalysts M_1/M_2 and C_3/C_4 indicates that the catalysts M_1 and C_3 bearing methyl groups on C–C backbone affording high level of SCB and also for stereoisomers of C_3 (active species), the behaviors are similar to that of mononuclear M_1.

Rigidity of the bridge is another controlling factor of catalyst behavior. Based on this, by increasing the flexibility of bridge structure (C_6), not only the broadening of MWD decreased but also the difference between the SCB formations of stereoisomers was reduced. The results were also confirmed by theoretical calculations where the energy interval between the stereoisomer structures decreased. Detailed microstructural characteristics of the polyethylene obtained using mononuclear (M_2) and dinuclear (C_2) catalysts were determined using ^{13}C NMR analysis.[35,56,57] As can be observed in Figure 5, the spectra in regard to chemical shifts are mostly similar except branching distribution (Table 2). Interestingly, the microstructure of the sample 4 contains rather a high level of hexyl (He) branches while for the sample 2, shorter chain branches are dominant. As we previously reported a high level of chain walking of dinuclear catalyst C_2 in polymerization of higher α-olefins (1-octene), it also may be suggested for the polymerization of ethylene that a high level of chain walking on macromonomer could lead to higher linearity in comparison to amorphous sample 2. In other side, high level of He branches could be a result of propagation along with agostic interaction of generated 1-octene and the second metal center. Based on this, a possible mechanism for the observed results is presented in Figure 6.

Also, regiorandom selectivity in branching distribution by M_2 could be observed, while for C_2 linearity of

TABLE 2 Branching density and distribution of samples 2 and 4

Sample	Branching density (per 1000 C)	Branching distribution (%)					
		Me	Et	Pr	Bu	He	L
2	75.2	50.8	11.6	12.7	13.0	2.4	9.5
4	39.6	41.2	7.6	7.0	14.1	19.4	10.7

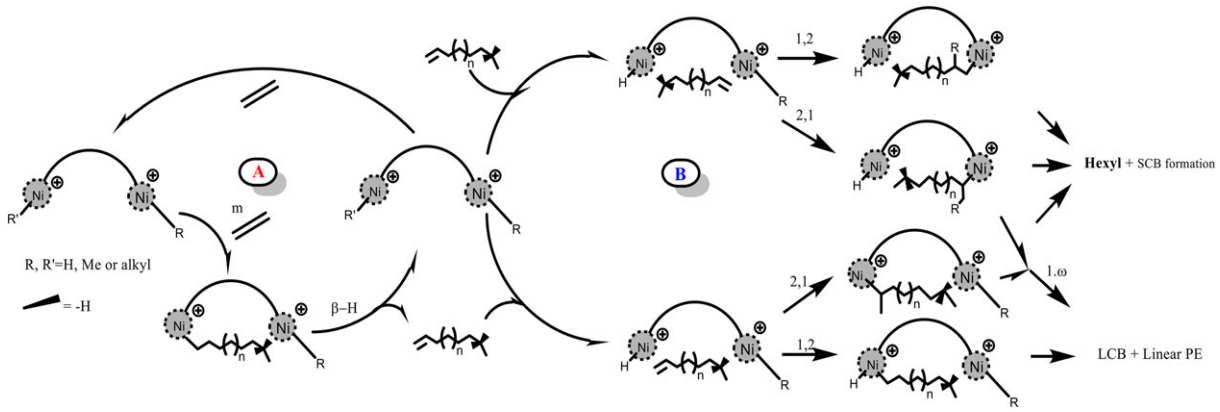

FIGURE 6 Proposed mechanism for branch formation by dinuclear catalysts

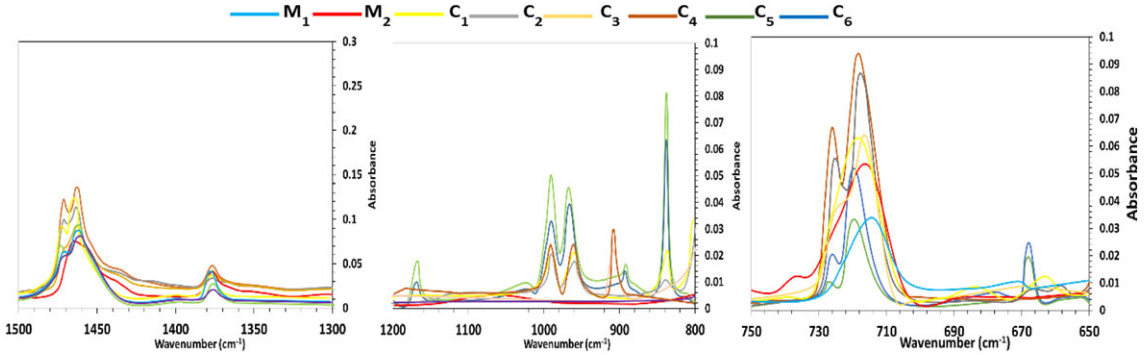

FIGURE 7 FT-IR spectra of polyethylene samples obtained using mononuclear (M_1 and M_2) and dinuclear (C_1–C_6) catalysts

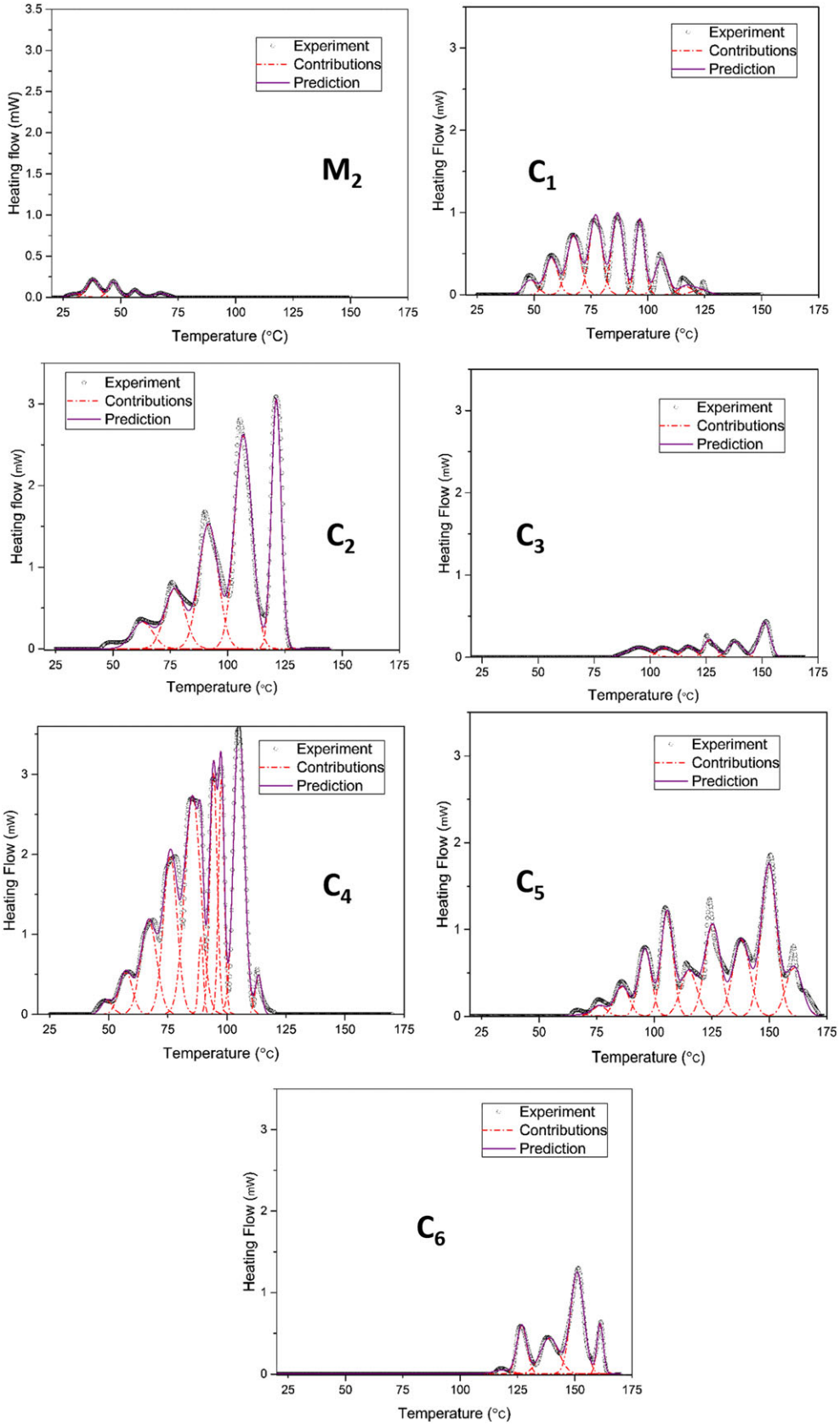

FIGURE 8 Fractionated melting endotherms of polyethylene obtained using mononuclear (M_2) and dinuclear (C_1–C_6) catalysts

polymer chain is observed along with a selectivity of He branches.

The proposed mechanism depicted in Figure 6 can be interpreted in terms of α-olefin formation (Figure 6, part A) for C_2 ($n = 1$) and following insertions and enchainments (Figure 6, part B) that lead to longer branches and chain straightening in comparison to M_2.

In addition, FT-IR spectra (Figure 7) showed some outstanding evidence regarding the microstructure of the samples.[43,58–60] For instance, bands at 717 cm^{-1} are indicative of the long-chain branches (≥He) which for the polyethylene made using catalysts C_1–C_4 could be observed and for C_2 and C_4 were much stronger, while for C_5 and C_6, bands at 841, 973–997 and 1162 cm^{-1} show the high level of methyl branches. Flexible and short distance between the Ni centers along with lower electronic effects provided by aliphatic bridges in C_5 and C_6 led to high level of short branching density (especially methyl branches). β-Hydrogen elimination and 2,1-insertion could lead to methyl branches. The ratio of the bands at 1378 and 1464 cm^{-1} is also useful for comparison of branching extent in microstructure of samples that is in accordance with GPC-IR and NMR results. Besides, unsaturation content of the polymer chain obtained through GPC-IR (0.3/1000 C and 0.5/1000 C for C_3 and C_4) in solution state was confirmed by FT-IR analysis in solid film. The peak at 908 cm^{-1} indicated the vinyl content in the microstructure of the samples. It could be suggested that long distance between the Ni centers and less shielding effect of *ortho* positions in catalysts C_3 and C_4 in comparison to C_1 and C_2, respectively, could lead to lower effective agostic interaction between the macromonomer and second Ni center leading to diffusion of vinyl chain into solution (Figure 6, part A).

These microstructural details could be observed in the thermal behavior of the samples. Thermal analysis is one of the most useful and promising methods for obtaining details of the microstructure and chemical composition of ethylene/α-olefin (co)polymers. For instance, SSA is a faster alternative for TREF and CRYSTAF, with higher sensitivity to both intra- and intermolecular heterogeneities of comonomer distribution.[61] On the other hand, late transition metal catalysts, especially Ni and Pd, are known as catalysts for production of highly branched polyethylene (chain walking mechanism instead of comonomer). These features can be observed for the polyethylene obtained using M_1 and M_2 that do not show any melting in DSC thermograms. Weighted summation of Gaussian distribution functions is used for deconvoluting the contribution of different lamella thicknesses.[50] For sample 2, a series of weak endotherms at low temperatures were observed (Figure 8) through the SSA technique, while for sample 1 crystallinity is not observed. As a result, catalyst M_1 produces highly branched polyethylene without any significant methylene disclosing very short methylene sequences. This thermal behavior is consistent with the NMR and FT-IR sequences and M_2 through lower SCBs in microstructure and weak endotherms at low temperature results. On the other hand, it can be observed in melting endotherms (SSA) of the polyethylene obtained using the dinuclear catalysts that there is heterogeneity of crystalline phase in samples 3 and 5–8, due to different chemical composition and broad MWD, while for the samples produced using C_2, homogeneity reveals much more uniform behavior of the catalyst in regard to SCB formation and methylene sequences. Intensities and regular linearity features allow the chains to form different and uniform domains of crystallinity. For the other dinuclear catalysts, in fact, the presence of second polyethylene phase could cause a disruption in crystallization or overlapping of endotherms. However, C_3 in comparison to C_4 afforded some weak endotherms at higher temperatures (Figure 8). In comparison to M_2, C_2 led to less branching content and higher melting temperature. This can be attributed to higher SCB content of polymer chain incorporated in crystalline phase. Interestingly, for the samples obtained using C_5 and C_6, high level of methyl branches incorporated in crystallization led to fractions with high melting temperature indicating ethylene/propylene copolymer analogues.

4 | CONCLUSIONS

In addition to the ligand backbone, the presence of a second metal center could change the catalyst behavior. This trend could be controlled by the nature and length of bridge between the active centers. These structural features, moreover, have an effect on the stability and activity of the catalyst and on polymer properties. Higher electron density provided by longer and bulkier groups on the ligand led to higher stability and activity of the dinuclear catalysts. Besides, the optimum bulkiness obtained by isopropyl and methyl substituents at *ortho* positions in catalyst C_2 afforded the highest performance. Theoretical parameters such as energy intervals and Mulliken charge on Ni atoms confirmed the experimental results. Regarding the thermal and microstructural properties of the polyethylene obtained using the mononuclear and dinuclear catalysts, M_1 and M_2 polymerized ethylene to a highly branched amorphous polyethylene, while for the dinuclear catalysts the results were different. Although the mononuclear catalysts did not show a specific selectivity of microstructure, the dinuclear catalysts exhibited superior control of polymer architecture. To clarify, catalyst C_2 demonstrated a selectivity of hexyl

branches, catalysts C_5 and C_6 led to an ethylene/propylene analogue through high level of methyl branches, and catalysts C_3 and C_4 afforded vinyl-terminated microstructure. Homogeneity and heterogeneity in polyethylene chains of the samples were observed through the SSA technique, MWD and SCB curves. Different trends for each catalyst were attributed to *syn* and *anti* stereoisomers. In addition, thermal behavior of the samples in the SSA technique exhibited different orders and intensities from methylene sequences and lamella thickness in respect of each stereoisomer behavior. Kinetic profiles of polymerization along with the computations showed that the short energy interval (activation energy) of precatalyst and catalyst leads to fast and higher activation rate (catalyst M_2), and strong interaction of ethylene and catalyst leads to high monomer uptake and productivity (catalyst C_2). Moreover, theoretical parameters including electron affinity, Mulliken charge on Ni, chemical potential and hardness, and global electrophilicity showed optimum values for C_2.

ACKNOWLEDGEMENTS

The authors are grateful to the University of Alberta (U of A), Iran Polymer and Petrochemical Institute (IPPI) and Ferdowsi University of Mashhad (FUM) for their cooperation. We also are grateful of Dr. Saeid Mehdiabadi and Mr. Vahid Vajihinejad for assistance with characterization.

ORCID

Mostafa Khoshsefat https://orcid.org/0000-0003-4461-8657
Saeid Ahmadjo https://orcid.org/0000-0002-8536-115X
Gholamhossein Zohuri https://orcid.org/0000-0003-2380-8363

REFERENCES

[1] M. Delferro, T. J. Marks, *Chem. Rev.* **2011**, *111*, 2450.
[2] W. Tao, S. Akita, R. Nakano, S. Ito, Y. Hoshimoto, S. Ogoshi, K. Nozaki, *Chem. Commun.* **2017**, *53*, 2630.
[3] M. R. Salata, T. J. Marks, *Macromolecules* **2009**, *42*, 1920.
[4] S. Liu, A. Motta, A. R. Mouat, M. Delferro, T. J. Marks, *J. Am. Chem. Soc.* **2014**, *136*, 10460.
[5] J. P. McInnis, M. Delferro, T. J. Marks, *Acc. Chem. Res.* **2014**, *47*, 2545.
[6] X. Xiao, J. Sun, X. Li, Y. Wang, H. Schumann, *Eur. Polym. J.* **2007**, *43*, 164.
[7] C. Görl, H. G. Alt, *J. Organometal. Chem.* **2007**, *692*, 5727.
[8] H. Alshammari, H. G. Alt, *Polyolefins J.* **2014**, *1*, 107.
[9] G. J. M. Meppelder, H. T. Fan, T. P. Spaniol, J. Okuda, *Inorg. Chem.* **2009**, *48*, 7378.
[10] M. P. Weberski, C. Chen, M. Delferro, T. J. Marks, *Chem. Eur. J.* **2012**, *18*, 10715.
[11] Y. Na, X. Wang, K. Lian, Y. Zhu, W. Li, Y. Luo, C. Chen, *ChemCatChem* **2017**, *9*, 1062.
[12] R. Wang, X. Sui, W. Pang, C. Chen, *ChemCatChem.* **2016**, *8*, 434.
[13] T. Sun, Q. Wang, Z. Fan, *Polymer* **2010**, *51*, 3091.
[14] Q. Xing, T. Zhao, Y. Qiao, L. Wang, C. Redshaw, W. H. Sun, *RSC Adv.* **2013**, *3*, 26184.
[15] F. Lindenberg, T. Shribman, J. Sieler, E. Hey-Hawkins, M. S. Eisen, *J. Organometal. Chem.* **1996**, *515*, 19.
[16] B. K. Bahuleyan, K. J. Lee, S. H. Lee, Y. Liu, W. Zhou, I. Kim, *Catal. Today* **2011**, *164*, 80.
[17] J. Gao, B. Yang, C. Chen, *J. Catal.* **2019**, *369*, 233.
[18] M. Chen, C. Chen, *Angew Chem Int Ed.* **2018**, *12*, 3094.
[19] K. Lian, Y. Zhu, W. Li, S. Dai, C. Chen, *Macromolecules* **2017**, *50*, 6074.
[20] R. Mundil, S. Hermanová, M. Peschel, A. Lederer, *Polym. Int.* **2018**, *67*, 946.
[21] C. Chen, *Nat. Rev. Chem.* **2018**, *2*, 6.
[22] C. Chen, *ACS Catal.* **2018**, *8*, 5506.
[23] S. Dai, C. Chen, *Macromolecules* **2018**, *51*, 6818.
[24] Y. Na, S. Dai, C. Chen, *Macromolecules* **2018**, *51*, 4040.
[25] S. Zhou, C. Chen, *Sci. Bull.* **2018**, *63*, 441.
[26] D. Zhang, C. Chen, *Angew. Chem.* **2017**, *129*, 14864.
[27] Y. Na, D. Zhang, C. Chen, *Polym. Chem.* **2017**, *8*, 2405.
[28] B. Yang, S. Xiong, C. Chen, *Polym. Chem.* **2017**, *8*, 6272.
[29] X. Sui, C. Hong, W. Pang, C. Chen, *Mater. Chem. Front.* **2017**, *1*, 967.
[30] J. Fang, X. Sui, Y. Li, C. Chen, *Polym. Chem.* **2018**, *9*, 4143.
[31] C. Zou, S. Dai, C. Chen, *Macromolecules* **2017**, *51*, 49.
[32] C. Rong, F. Wang, W. Li, M. Chen, *Organometallics* **2017**, *36*, 4458.
[33] S. Tian, Y. Zhang, R. Li, F. Wang, W. Li, *Inorg. Chim. Acta* **2019**, *486*, 492.
[34] F. Wang, R. Tanaka, Z. Cai, Y. Nakayama, T. Shiono, *Polymer* **2016**, *8*, 160.
[35] F. Wang, R. Li, S. Tian, K. Lian, D. Guo, W. Li, *Appl. Organometal. Chem.* **2018**, *32*, e4298.
[36] J. M. Benito, E. de Jesús, F. J. de la Mata, J. C. Flores, R. Gómez, P. Gómez-Sal, *Organometallics* **2006**, *25*, 3876.
[37] L. Zhu, Z. S. Fu, H. J. Pan, W. Feng, C. Chen, Z. Q. Fan, *Dalton Trans.* **2014**, *43*, 290.
[38] J. D. Pelletier, J. Fawcett, K. Singh, G. A. Solan, *J. Organometal. Chem.* **2008**, *693*, 2723.
[39] S. Jie, D. Zhang, T. Zhang, W. H. Sun, J. Chen, Q. Ren, W. Chen, *J. Organometal. Chem.* **2005**, *690*, 1739.
[40] S. Zhang, W. H. Sun, X. Kuang, I. Vystorop, J. Yi, *J. Organometal. Chem.* **2007**, *692*, 5307.
[41] S. Kong, K. Song, T. Liang, C. Y. Guo, W. H. Sun, C. Redshaw, *Dalton Trans.* **2013**, *42*, 9176.
[42] H. K. Luo, H. Schumann, *J. Mol. Catal. Chem.* **2005**, *227*, 153.
[43] M. Khoshsefat, G. H. Zohuri, N. Ramezanian, S. Ahmadjo, M. Haghpanah, *J. Polym. Sci. A* **2016**, *54*, 3000.

[44] D. A. Ferreira, F. D. A. Sara, S. M. Meneghetti, M. R. Meneghetti, *J. Mol. Catal. Chem.* **2012**, *363*, 1.

[45] J. Ramos, A. Muñoz-Escalona, V. Cruz, J. Martínez-Salazar, *Polymer* **2003**, *44*, 2177.

[46] S. Kong, C. Y. Guo, W. Yang, L. Wang, W. H. Sun, R. Glaser, *J. Organometal. Chem.* **2013**, *725*, 37.

[47] T. Zhang, W. H. Sun, T. Li, X. Yang, *J. Mol. Catal. Chem.* **2004**, *218*, 119.

[48] X. Zhang, B. Duan, W. Sun, S. L. Hsu, X. Yang, *Sci China Ser. B.* **2009**, *52*, 48.

[49] S. Mehdiabadi, J. B. Soares, *Macromolecules* **2016**, *49*, 2448.

[50] M. Ahmadi, R. Rashedi, S. Ahmadjo, M. Karimi, M. Zahmaty, S. M. M. Mortazavi, *J. Therm. Anal. Calorim.* **2018**, *131*, 2523.

[51] M. Khoshsefat, S. Ahmadjo, S. M. M. Mortazavi, G. H. Zohuri, J. B. P. Soares, *New J. Chem.* **2018**, *42*, 8334.

[52] A. Dechal, M. Khoshsefat, S. Ahmadjo, S. M. M. Mortazavi, G. H. Zohuri, H. Abedini, *Appl. Organometal. Chem.* **2018**, *32*, e4355.

[53] M. Khoshsefat, A. Dechal, S. Ahmadjo, S. M. M. Mortazavi, G. H. Zohuri, J. B. P. Soares, *New J. Chem.* **2018**, *42*, 18288.

[54] S. Mehdiabadi, J. B. Soares, *Macromolecules* **2012**, *45*, 1777.

[55] S. A. Svejda, L. K. Johnson, M. Brookhart, *J. Am. Chem. Soc.* **1999**, *121*, 10634.

[56] C. J. Stephenson, J. P. McInnis, C. Chen, M. P. Weberski Jr., A. Motta, M. Delferro, T. Marks, *ACS Catal.* **2014**, *4*, 999.

[57] G. B. Galland, R. F. de Souza, R. S. Mauler, F. Nunes, *Macromolecules* **1999**, *32*, 1620.

[58] M. R. Jung, F. D. Horgen, S. V. Orski, V. Rodriguez, K. L. Beers, G. H. Balazs, K. D. Hyrenbach, *Mar. Pollut. Bull.* **2018**, *127*, 704.

[59] R. C. Asensio, M. S. A. Moya, J. M. de la Roja, M. Gómez, *Anal. Bioanal. Chem.* **2018**, *395*, 2081.

[60] A. Malmberg, E. Kokko, P. Lehmus, B. Löfgren, J. V. Seppälä, *Macromolecules* **1998**, *31*, 8448.

[61] M. Karimi, S. M. M. Mortazavi, S. Ahmadjo, M. Ahmadi, *Polym. Adv. Technol.* **2018**, *29*, 1161.

How to cite this article: Khoshsefat M, Dechal A, Ahmadjo S, Mortazavi SMM, Zohuri G, Soares JBP. Cooperative effect through different bridges in nickel catalysts for polymerization of ethylene. *Appl Organometal Chem*. 2019;e4929. https://doi.org/10.1002/aoc.4929